

Nonlinear supratransmission as a fundamental instability

Jérôme LEON

Physique Mathématique et Théorique, CNRS-UMR 5825
34095 MONTPELLIER (FRANCE)

Abstract

The *nonlinear supratransmission* is the property of a nonlinear system possessing a natural forbidden band gap to transmit energy of a signal with a frequency in the gap by means of generation of nonlinear modes (gap solitons). This process is shown to result from a generic instability of the evanescent wave profile generated in a nonlinear medium by the incident signal.

1 Introduction

A plane wave scattering onto a medium which possess a natural forbidden band gap, is totally reflected if its frequency falls in the gap. Such may not be the case if the medium is nonlinear, as the sine-Gordon model considered in [1] where the incident wave was shown to generate, above some amplitude threshold, a sequence of nonlinear modes propagating in the medium.

This threshold was given an analytic expression in [2] (still in the sine-Gordon case) and the property of the nonlinear medium to transmit energy in the gap has been called *nonlinear supratransmission*. It has been shown then to hold for different models (nonlinear Klein-Gordon, double sine-Gordon, Josephson transmission lines), and has been experimentally realized on a chain of coupled pendula [3].

Energy transmission by gap soliton generation is a phenomenon that has been experimentally discovered in Bragg media with Kerr nonlinearity [4]. In that case the underlying simplified model is the *coupled mode system* [5] and it has been recently demonstrated that the very mechanism of the switch from a Bragg mirror to a medium with high transmissivity is the nonlinear supratransmission [6]. Again there the theory allows for an analytic expression of the threshold amplitude, based on the expression of the soliton solution of the coupled mode system found in [7].

We demonstrate here that the process of nonlinear supratransmission is a natural consequence of a generic instability of the evanescent profile generated

in a nonlinear medium when it is constrained at one end by a periodic boundary driving of frequency in a forbidden band gap.

2 General context

Let us consider the Lagrangian of a scalar field $u(x, t)$ in the half-plane $(x, t) \in \mathbb{R}^+ \times \mathbb{R}$

$$\mathcal{L} = \int_0^\infty dx L(u, u_t, u_x) , \quad L = \frac{1}{2}u_t^2 - \frac{1}{2}u_x^2 - \phi(u) . \quad (1)$$

The equation of motion $\delta\mathcal{L} = 0$ reads

$$x > 0 : u_{tt} - u_{xx} + \phi'(u) = 0 , \quad (2)$$

where *prime* denotes differentiation with respect to the argument. The wave equation (2) is submitted to Dirichlet boundary conditions

$$u(0, t) = f(t) , \quad u(\infty, t) = 0 , \quad (3)$$

associated with Cauchy initial data $u(x, 0)$ and $u_t(x, 0)$, which can be vanishing or adapted to the boundary forcing. Note that this approach can be extended to Neumann boundary conditions.

From now on we adopt the quite generic assumption of a potential energy $\phi(u)$ which possess a local minimum locally symmetric. By a convenient choice of the reference frame, this minimum can be taken to be located at $(\phi, u) = (0, 0)$. Then the symmetric requirement means that the potential is *locally* an even function of u . Moreover, by a convenient choice of the units of x and t we can always scale the value of $\phi''(0)$ to the value 1. In summary the potential $\phi(u)$ obeys the following requirements

$$\phi(0) = 0 , \quad \phi'(0) = 0 , \quad \phi''(0) = 1 , \quad \phi'''(0) = 0 . \quad (4)$$

Note that the *local parity assumption* $\phi'''(0) = 0$ is not essential but simplifies the expressions.

As a consequence the equation (2), by Taylor expansion of $\phi'(u)$ about the minimum $u = 0$, has the linear limit

$$u_{tt} - u_{xx} + u = 0 , \quad (5)$$

with dispersion relation

$$\omega^2 = 1 + k^2 , \quad (6)$$

having the gap $[-1, +1]$ in the frequency.

The second restriction is on the class of boundary datum $f(t)$ which we take to be a periodic forcing with a frequency belonging to the forbidden band gap. More precisely we assume

$$u(0, t) = A \cos(\Omega t) , \quad |\Omega| < 1 . \quad (7)$$

This problem is quite generic and describes e.g. the scattering of a monochromatic wave into a medium in one of its forbidden band gaps.

For the linear limit (5), the boundary condition (7) would generate the solution ($x > 0$)

$$u_0(x, t) = A \cos(\Omega t) e^{-Kx} , \quad \Omega^2 = 1 - K^2 , \quad (8)$$

called the linear evanescent wave. This solution is a reasonable approximate solution of the nonlinear evolution as long as the amplitude A is small enough.

We show hereafter that in the nonlinear case, under some additional simple conditions on the potential $\phi(u)$, the medium can present *nonlinear supratransmission* as a result of a fundamental instability generated by the evanescent wave, above some threshold for the amplitude A .

3 Perturbation scheme

Let us start with the simplest nonlinear correction resulting from the assumption (4), namely the nonlinear wave equation

$$u_{tt} - u_{xx} + u + \frac{1}{6}\alpha u^3 = 0 , \quad (9)$$

where the nonlinear factor α is defined by

$$\alpha = \left. \frac{\partial^4 \phi}{\partial u^4} \right|_{u=0} . \quad (10)$$

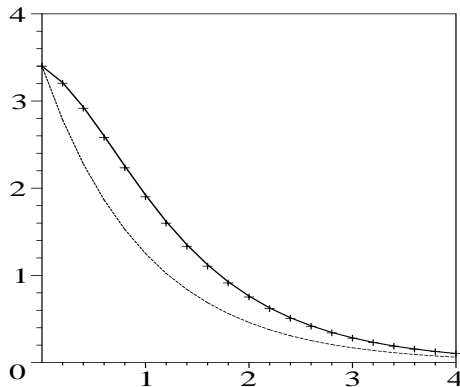


Figure 1: Plot of the actual nonlinear evanescent profile $u_1(x)$ (full line) compared to the linear one $u_0(x)$ (dashed line) in the static case $\Omega = 0$ for $A = 3.4$. The dots are the results of a numerical simulation of (9).

It is essential to remark at this step that the first effect of the nonlinearity on a boundary driving (7) is to *deform* the (linear) evanescent profile (8). Such

a deformation can be illustrated analytically and numerically in the static case $\Omega = 0$ in (7). Indeed the equation (9) with $\alpha = -1$ for $u(x)$ submitted to $u(0) = A$, possess the solution

$$u_1(x) = \frac{2\sqrt{3}}{\cosh(x - x_0)}, \quad x_0 = -|\operatorname{arccosh}(\frac{2\sqrt{3}}{A})|. \quad (11)$$

This is the profile displayed on the figure 1 with $A = 3.4$ (full line) in perfect agreement to numerical simulations (dots). The numerical method is explained in the appendix and here we have solved (9) with a boundary datum $u(0, t)$ slowly increasing from 0 to the value $A = 3.4$ and the solution (represented by the crosses in fig. 1) is plotted long after the boundary datum has been setted. We have plotted also for comparison to the exponential (linear) shape (8) namely $u_0(x) = Ae^{-x}$ (dashed line).

In the dynamical case ($\Omega \neq 0$) we denote by $u_1(x, t)$ the *deformed evanescent profile*, solution of (9), hence required to obey the boundary value (7), namely

$$u_1(0, t) = A \cos(\Omega t). \quad (12)$$

Although this solution $u_1(x, t)$ may not be known analytically, we shall actually discover that the worst approximation of it, namely the linear evanescent profile $u_0(x, t)$ itself, still generates the seeked instability, hence providing a qualitative understanding of the generation of nonlinear supratransmission.

4 Instability criterion

The second effect of the boundary driving is obtained by studying the perturbation of the exact solution $u_1(x, t)$ of (9) as

$$u(x, t) = u_1(x, t) + \epsilon \eta(x, t), \quad \epsilon \ll 1. \quad (13)$$

At order ϵ , the evolution for the perturbation η then reads

$$x > 0, \quad \eta_{tt} - \eta_{xx} + \eta[1 + V] = 0, \quad V(x, t) = \frac{1}{2}\alpha u_1^2(x, t). \quad (14)$$

This linear wave equation in the potential V on the semi-axis $x > 0$ is our main tool and contains all the ingredients required for a qualitative description of the onset of instability.

The linear equation (14) can be thought of as a two-dimensional scattering problem on the half-plane for a potential which is periodic in the infinite t -dimension and localized around $x = 0$ in the positive x -direction. The study of this mixed periodic-localized 2D scattering problem is a tough technical question that we report in a future investigation.

However we show hereafter that the instability can be qualitatively understood by considering the *static case* where V is assumed to depend only on the

space variable x . The scattering problem can then be reduced to the radial S-wave Schrödinger spectral problem

$$\psi_{xx}(\zeta, x) + [(\lambda^2 - 1) - V(x)] \psi(\zeta, x) = 0 , \quad (15)$$

for the spectral parameter ζ and eigenfunction $\psi(\zeta, x)$ defined by

$$\zeta^2 = \lambda^2 - 1 , \quad \eta(x, t) = e^{i\lambda t} \psi(\zeta, x) . \quad (16)$$

We argue then that equation (14) develops an instability if the potential V possess a bound state, say $\zeta = ip$, with *sufficient energy*, namely if

$$\zeta^2 = -p^2 , \quad p > 1 \Rightarrow \lambda^2 < 0 , \quad (17)$$

which causes the first order correction $\eta(x, t)$ to diverge in time. In particular it is clear from (14) that the instability will develop only when $\alpha < 0$ as a necessary (not sufficient) condition to have a bound state for V . In order to allow for a comparison with sine-Gordon, and because the value of α in (9) can be scaled with A , we set

$$\alpha = -1 . \quad (18)$$

The potential $V(x)$ is obtained from the *deformed evanescent profile* $u_1(x, t)$ by considering its extremum on a period, namely we take

$$V(x) = -\frac{1}{2} \max_t \{u_1^2(x, t)\} . \quad (19)$$

We now illustrate the obtained expression for the threshold of instability for two particular choices for u_1 , first the linear evanescent profile (8), second a standard sech-type profile. Both cases allow for an explicit computation of this threshold and we compare in figure 2 these results to numerical simulation of the PDE (9).

5 The exponential potential

The choice $A \exp[-Kx]$ for $\max\{u_1^2(x, t)\}$ provides from (15) the following spectral problem on the half-line

$$x > 0 , \quad \psi_{xx}(\zeta, x) + \left[\zeta^2 + \frac{1}{2} A^2 e^{-2Kx} \right] \psi(\zeta, x) = 0 . \quad (20)$$

The two (positive, real-valued) parameters are the amplitude A and the *wave number* $K = \sqrt{1 - \Omega^2}$.

The direct scattering problem [8, 9] essentially consists in finding the Jost solution of (20) which can be written

$$f(\zeta, x) = e^{i\zeta x} {}_0F_1\left(1 - i\frac{\zeta}{K}; -\frac{A^2}{8K^2} e^{-2Kx}\right) . \quad (21)$$

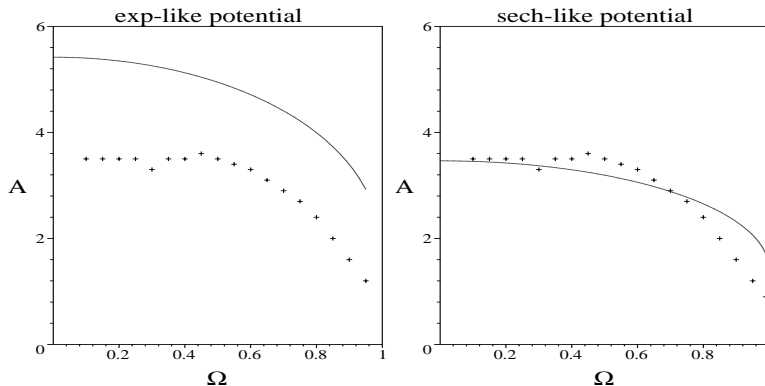


Figure 2: Comparison of the threshold of instability for the full equation (9) (crosses) with the theory obtained from (14) with $\alpha = -1$ for $u_1 = A \exp[-Kx]$ (full line left figure) and $u_1 = A / \cosh(Kx)$ (full line right figure).

This solution is usually written in terms of the Bessel function of the first kind of order $-i\zeta/K$. We find it more convenient to express it in terms of the generalized hypergeometric function ${}_0F_1$. Indeed it readily provides the asymptotic behavior

$$f(\zeta, x)e^{-i\zeta x} \xrightarrow{x \rightarrow \infty} 1, \quad (22)$$

and the Jost function

$$f(\zeta, 0) = {}_0F_1\left(1 - i\frac{\zeta}{K}; -\frac{A^2}{8K^2}\right). \quad (23)$$

The bound states are the zeroes of this Jost function in the upper complex ζ -plane, actually located on the imaginary axis as the potential is real valued. Our instability criterion (17) then tells that an instability for $\eta(x, t)$ will develop as soon as the amplitude A reaches the value A_s for which the first bound state reaches the value $\zeta = i$. This occurs for each value of the parameter K and thus the threshold $A_s(K)$ is defined by the implicit equation

$${}_0F_1\left(1 + \frac{1}{K}; -\frac{A_s^2}{8K^2}\right) = 0. \quad (24)$$

We have solved this equation numerically and the result is plotted in terms of $\Omega = \sqrt{1 - K^2}$ in the left figure 2.

It is compared there with the results of the numerical solution (see appendix) of (9) (with $\alpha = -1$) submitted to the boundary driving (7), namely $u(0, t) = A \cos \Omega t$. Although the theoretical threshold does not fit perfectly the simulations, the principle of the nonlinear supratransmission is qualitatively understood. The discrepancy results both from the assumption of an exponential profile for $u_1(x, t)$ and a static approximation of it.

6 The Eckart potential

A better fit is obtained by assuming instead of the exponential profile the following sech-type profile obtained from the solution (11) at its maximum amplitude (i.e. for $x_0 = 0$ where the instability is expected)

$$u_1 = \frac{A}{\cosh Kx}, \quad K = \sqrt{1 - \Omega^2}. \quad (25)$$

The presence of a periodic boundary datum is taken into account by the parameter K (wave number). This choice is expected to give good results for small Ω and it leads to the spectral problem

$$x > 0, \quad \psi_{xx}(\zeta, x) + \left[\zeta^2 + \frac{1}{2} \frac{A^2}{\cosh^2 Kx} \right] \psi(\zeta, x) = 0. \quad (26)$$

This potential belongs to the Eckart class [8] and its Jost solution reads

$$f(\zeta, x) = e^{i\zeta x} (1 + e^{-2Kx})^\beta {}_2F_1(\beta, \beta - i\frac{\zeta}{K}; 1 - i\frac{\zeta}{K}; -e^{-2Kx}), \quad (27)$$

with the parameter

$$\beta = \frac{1}{2} \left(1 - \sqrt{1 + 2A^2/K^2} \right). \quad (28)$$

This solution does obey the asymptotic (22) and the Jost function is

$$f(\zeta, 0) = 2^\beta {}_2F_1(\beta, \beta - i\frac{\zeta}{K}; 1 - i\frac{\zeta}{K}; -1). \quad (29)$$

According to the instability criterion (17) we then seek the value A_s for the threshold amplitude generating a bound state (zero of this Jost function on the upper imaginary ζ -axis) at the value $\zeta = i$. From [10] we can write also (29) as

$$f(\zeta, 0) = \frac{2^{i\zeta/K} \sqrt{\pi} \Gamma(1 - i\frac{\zeta}{K})}{\Gamma(\frac{1+\beta}{2} - i\frac{\zeta}{2K}) \Gamma(1 - \frac{\beta}{2} - i\frac{\zeta}{2K})}, \quad (30)$$

where $\Gamma(v)$ is the standard Euler Gamma function that possess poles at $v = 0, -1, \dots$.

The bound states are thus given by the poles of the function $\Gamma(\frac{1+\beta}{2} - i\frac{\zeta}{2K})$ on the positive imaginary ζ -axis, and the first bound state reaches the point $\zeta = i$ as soon as β verifies

$$\frac{1+\beta}{2} + \frac{1}{2K} = 0. \quad (31)$$

Replacing there the value (28) of the parameter β , the threshold of instability A_s can then be expressed in terms of $\Omega = \sqrt{1 - K^2}$ as

$$A_s^2 = 4(1 - \Omega^2) + 6\sqrt{1 - \Omega^2} + 2. \quad (32)$$

This is the curve represented in the right graph of figure 2. We see then that the sech-like profile provides as expected a much better fit of the instability threshold, especially for small Ω where the static approximation becomes more accurate.

7 The sine-Gordon case

So far we have demonstrated the existence of an onset of instability in the nonlinear simple model (9) (with $\alpha < 0$). In that case the instability causes the solution to diverge because the related potential $\phi(u) = u^2/2 - u^4/24$ is not confining for large u .

To illustrate the nonlinear supratransmission as an effect of the instability, we consider now the sine-Gordon case $\phi(u) = 1 - \cos(u)$ treated in [2, 3], namely

$$x > 0 : \quad u_{tt} - u_{xx} + \sin u = 0, \quad u(0, t) = A \cos \Omega t. \quad (33)$$

In this situation, the solution induced by the boundary datum of amplitude *below* the threshold of instability is the *non-travelling* breather

$$u_b(x, t) = 4 \arctan \left[\frac{K}{\Omega} \frac{\cos(\Omega t)}{\cosh(K(x - x_b))} \right], \quad x_b < 0, \quad (34)$$

where x_b is the breather center.

The onset of nonlinear supratransmission is reached, at given frequency Ω , for the maximum amplitude of $u_b(0, t)$, obtained of course for $x_b = 0$. Let $u_2(x, t)$ denote the solution u_b for $x_b = 0$, namely

$$u_2(x, t) = 4 \arctan \left[\frac{K}{\Omega} \frac{\cos(\Omega t)}{\cosh(Kx)} \right]. \quad (35)$$

The first order perturbation $\epsilon \eta(x, t)$ about the solution u_2 obeys from (33) the linear evolution

$$x > 0, \quad \eta_{tt} - \eta_{xx} + \eta[1 + V] = 0, \quad V(x, t) = \cos(u_2) - 1. \quad (36)$$

that replaces equation (14) used precedingly. The potential V can also be written

$$V(x, t) = -8 \frac{K^2 \cos^2 \Omega t}{\Omega^2 \cosh^2 Kx} \left[1 + \frac{K^2 \cos^2 \Omega t}{\Omega^2 \cosh^2 Kx} \right]^{-2}. \quad (37)$$

Our purpose here is to show that the threshold of instability of the linear evolution (36) with the *stationary approximation* (19), namely

$$V(x) = -8 \frac{B^2}{\cosh^2 Kx} \left[1 + \frac{B^2}{\cosh^2 Kx} \right]^{-2}. \quad (38)$$

matches reasonably the theoretical prediction, namely the value B_s of the parameter B given from (37) by

$$B_s = \frac{K}{\Omega} = \frac{\sqrt{1 - \Omega^2}}{\Omega}. \quad (39)$$

The drawback here is that the potential (38) does not lead to an explicitly solvable spectral problem (15). This is why we have used numerical simulations

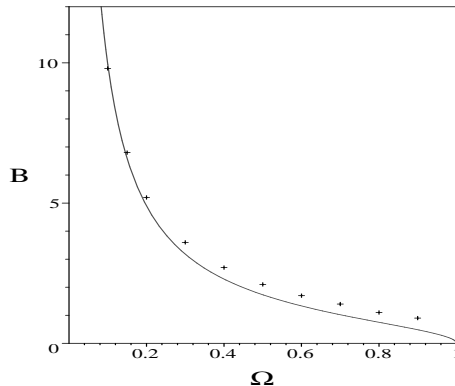


Figure 3: Onset of instability for the parameter B of $V(x)$ given by numerical simulations of (36) with (38) (dots) compared to the prediction (39).

and shown by figure 3 that the stationary limit does produce a consistent result: the threshold of instability of the PDE (36) obtained by varying B , at each fixed Ω , fits surprisingly well the exact prediction (39).

Note finally that in the sine-Gordon case we have an analytic expression of the threshold amplitude that generates nonlinear supratransmission [2], namely

$$A_s(\Omega) = 4 \arctan[\sqrt{1 - \Omega^2}/\Omega] . \quad (40)$$

This is simply the maximum amplitude of the breather (35), which is indeed reached when B in (38) takes the value (39). Above this value the instability comes into play and generates a nonlinear mode that propagates in the medium carrying energy, what have been called nonlinear supratransmission and have been experimentally realized on a chain of pendula [3].

8 Conclusion

We have demonstrated that a nonlinear medium, under some generic conditions on the structure of the nonlinearity (existence of a forbidden band gap, local minimum for the potential, ...) may create an instability of the evanescent profile generated by a periodic boundary driving at a frequency in the gap. This instability is the generating process at the origin of nonlinear supratransmission, when the nonlinear medium supports nonlinear modes (breathers, solitons, kinks, ...).

The instability has been described by using a stationary limit for the evanescent profile which has allowed us to prove that the occurrence of the instability is related to the appearance of a bound state with sufficient energy, according to (17).

We have dealt here with a scalar wave-like equation and it is worth mentioning that the process works also for different types of systems like for instance

the coupled mode equations in Bragg media [6]. The generating instability in this case will be considered in a future work.

A Numerical simulations

In order to integrate numerically the partial differential equations to deal with, we have used two different approaches depending whether the PDE is linear or not.

In the nonlinear case, such as equation (2), we have used an explicit second order scheme in space and solved for time evolution as a set of coupled differential equations. More precisely we have replaced (2) with the set of ODE's (overdot means time differentiation)

$$\ddot{u}_n - \frac{1}{h^2}(u_{n+1} - 2u_n + u_{n-1}) + \phi'(u_n) = 0, \quad n = 0..N, \quad (41)$$

where h is the chosen grid step and $u_n(t) = u(nh, t)$.

The boundary datum (7) is smoothly settled by assuming

$$u_0(t) = A \frac{1}{2} [1 + \tanh(p(t - t_0))] \cos \Omega t, \quad (42)$$

where p and t_0 are the parameters to select. A semi-infinite line is simulated by an absorbing end consisting of a damping term $\gamma \dot{u}_n$ included in the equation where the intensity γ slowly varies from 0 to 1 over the last 40 cells.

The results presented in figures 1 and 2 are obtained with $N = 100$ spatial mesh points, $h = 0.2$ grid spacing over a time of integration $t_m = 200$. The parameters for the boundary field are $p = 0.2$ and $t_0 = 20$. The resulting set of coupled ODEs is then solved through the subroutine `dsolve` of the `MAPLES` software package that uses a Fehlberg fourth/fifth order Runge-Kutta method.

In the linear case, namely for equation (36), we have used the `pdsolve` routine of `MAPLES` over a length $L = 10$ and a space-time step of 0.1. It uses a centered implicit scheme, of second order in space and time, with a first order boundary condition. To test the stability of an equation like (36) we have solved it for the following set of initial-boundary values

$$\eta(0, t) = 0.01, \quad \eta(L, t) = 0.01, \quad \eta(x, 0) = 0.01, \quad \eta_t(x, 0) = 0. \quad (43)$$

In the stable region we observe small amplitude oscillations that grow when the potential parameter get close to the instability threshold. Above this threshold the instability manifests as an exponential growth of the solution. The points that result in the figure 3 denote the first value of the parameter B for which instability settles in, with an absolute precision of 10^{-1} .

References

- [1] J-G. Caputo, J. Leon, A. Spire, Phys Lett A 283 (2001) 129

- [2] F. Geniet, J. Leon, Phys Rev Lett 89 (2002) 134102
- [3] F. Geniet, J. Leon, J Phys Cond Mat 15 (2003) 2933
- [4] D. Taverner, N.G.R. Broderick, D.J. Richardson, R.I. Laming, M. Ibsen, Opt Lett 23 (1998) 328
- [5] C. Martijn de Sterke, J.E. Sipe, Phys Rev A 38 (1988) 5149
- [6] J. Leon, A. Spire, *Gap soliton formation by nonlinear supratransmission in Bragg media*, preprint Montpellier 2003
- [7] A.B. Aceves, S. Wabnitz, Phys Lett A 14 (1989) 37
- [8] R.G. Newton, *Scattering theory of waves and particles*, McGraw-Hill (New-York 1966)
- [9] K. Chadan, P.C. Sabatier, *Inverse problems in quantum scattering theory*, Springer-Verlag (Berlin 1989)
- [10] A. Erdélyi, *Higher transcendental functions*, vol 1, McGraw-Hill (New-York 1953)